



# MEASUREMENT OF DAMAGE PROGRESSION IN OPEN HOLE TENSION TESTS

Adrian F Gill\*, Paul Robinson\*, Dennis Hitchings\*

\*Imperial College London

**Keywords:** *full strain field, open hole tension, damage progression*

## Abstract

*To be completely confident in the accuracy of a damage propagation model for composite structures it is necessary to validate the predicted behaviour against experimental results. It is therefore desirable to develop techniques for identifying and tracking damage as it progresses through laminated composite specimens. This has been achieved for open hole tension (OHT) coupons by employing a combination of full strain field measurement, acoustic emission, microscopy and ultrasound C-scan techniques.*

*Using this method, it has been possible to locate and distinguish damage by identifying areas that exhibit sudden increases in strain resulting from changes in laminate compliance. Correlation with recorded acoustic emission events and post-test microscopy was used to confirm that damage had occurred.*

*The work described in this paper provides a means for validating predictive models as well as helping to develop a better understanding of damage mechanisms.*

## 1 Introduction

Damage propagation models for composite materials are traditionally validated against experimental results using ultimate load and displacement. However, this method does not take into consideration the path of damage progression or the type of damage that occurred. Thus, to be completely confident in the accuracy of proposed damage models, it is necessary to develop techniques for identifying and tracking damage as it progresses through laminated composite structures.

A number of authors have investigated tracking damage progression using a variety of methods, most involving strain field techniques. Pierron *et al* [2] developed the Virtual Fields Method (VFM) that enables the parameters of the constitutive equations

to be determined from measured strain fields. In [2] this method was applied to glass/epoxy samples loaded in Iosipescu bending-shear. It was found that shear modulus ( $Q_{66}$ ) was accurately determined but the dominance of shear strain compared to the normal strains resulted in inaccuracies in  $Q_{11}$ ,  $Q_{22}$  and  $Q_{12}$ . Zhang *et al* [3] on the other hand applied the technique called thermographic stress analysis (TSA) to determine the effective modulus, mass density and damage parameter of glass/epoxy laminates. Good correlation with extensometer measurements was reported and a fatigue relationship between effective modulus, original modulus, number of damaging cyclic loads and peak nominal stress was developed. However, uncertainty still remains over the effect of thermal expansion coefficients, surface coating thickness and absolute temperature increase in the material due to cyclic loading. Ambu *et al* [4] used digital image correlation of random greyscale patterns to determine strain and displacement fields for static and fatigue tensile loading of graphite/PEEK and graphite/epoxy laminates. This technique enabled damage progression near the stress riser to be evaluated from the strain maps. In [5] the technique Electronic Speckle Pattern Interferometry (ESPI) involving simultaneous illumination of a speckle pattern by two symmetrically oriented laser beams is also shown to be suitable for determining strain fields of deformed composite laminates.

All of the above techniques are reported to be effective in locating damage and/or determining the degraded modulus. However, it is thought that there is a requirement to identify and verify the damage mechanisms responsible for the observed strain field changes as well as tracking the path of damage progression.

To achieve this, a combination of Digital Speckle Photogrammetry (DSP) strain field measurement, acoustic emission, microscopy and ultrasound C-scan techniques were employed for open hole tension (OHT) tests of 5-harness satin CFRP laminates.

## 2 Laminate Manufacture and Test Method

Quasi-isotropic 5-harness satin (5HS) woven carbon-fibre / epoxy resin laminates were manufactured by resin transfer moulding (RTM) and fabricated into OHT coupons according as per [1]. Laminates comprised 8-plyies (approx 62% fibre volume fraction) and were 2.8 mm thick. Coupon dimensions are shown in Fig. 1.

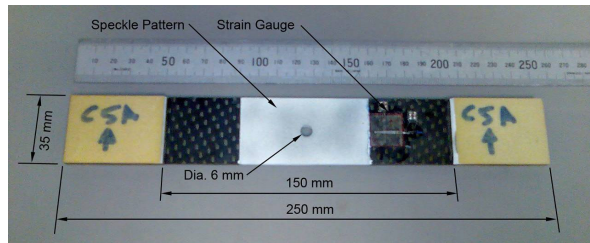


Fig. 1. OHT coupon with dimensions.

OHT tests were performed as per [1] (Fig. 2) and strain fields were recorded and computed using ARAMIS Digital Speckle Photogrammetry (DSP) equipment. DSP is an optical technique for computing strains and displacements by tracking a recognisable pattern spray-painted onto a surface. The ARAMIS software used in this investigation calculates the strain field by differentiating the displacements in two directions monitored by the camera for small facets automatically meshed onto the surface. Facet size for this investigation was approximately 0.5 mm x 0.5 mm (225 pixels per facet). Strain results for the system were verified with strain gauge data away from the hole and tabs and excellent correlation was found.



Fig. 2. Digital speckle photogrammetry (DSP) system

Tests were also monitored using a one sensor acoustic emission system to record damage events (hits), signal amplitude, duration, counts and energy.

## 3 Results

### 3.1 Location of Damage

All tested OHT specimens failed though a combination of fibre fracture, matrix cracking and delamination (Fig. 3). Fig. 4 shows the longitudinal strain field of such a specimen just before final failure occurs with the location of a significant change in strain identified. Fig. 5 presents the strain at the identified point over the duration of the test. It can be seen that at 275 seconds into the test a large increase in strain occurred. This increase in strain results from changes in the compliance of the laminate and is indicative of damage. The occurrence of damage at this stage in the test was confirmed by a large acoustic emission event (Fig. 6). Additionally, the occurrence of damage at the identified point was confirmed through post-test microsections such as Fig. 9.



Fig. 3. Failure of a quasi-isotropic OHT specimen.

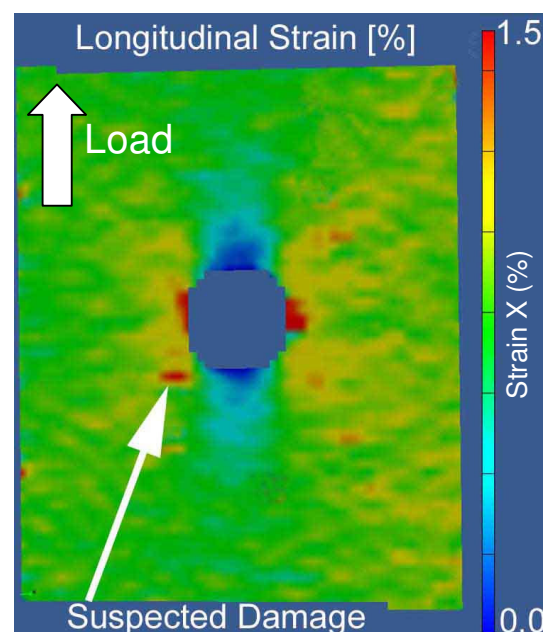


Fig. 4. Strain field with damage highlighted.

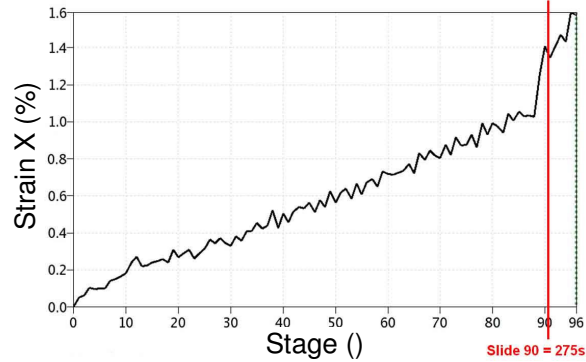


Fig. 5. Strain at highlighted damage point.

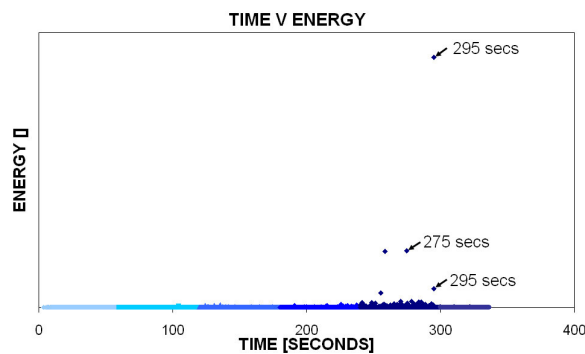


Fig. 6. AE output shows large emissions as 275 secs, corresponding to observed strain increase. Final failure occurred at 295 secs.

### 3.2 Identification of Damage Mechanism

To identify the damage mechanisms responsible for the observed strain increases, tests were repeated as per section 3.1 but stopped at significant acoustic emission bursts. It was found that observed strain increase could be assigned to one of three damage types (Fig. 13):

- The damage event suspected of being fibre fracture exhibited a sudden large strain increase. (Fig. 13 – Top)
- Suspected matrix cracking exhibited a sudden small strain increase. (Fig. 13 – Middle)
- Suspected stable delamination growth exhibited a long duration damage event of large magnitude. (Fig. 13 – Bottom)

The change in strain field between 413 secs and 444 secs in Fig. 13 (from two lobes to one) is the result of crack formation at about 8 o'clock to the hole (Fig. 8) that causes a redistribution of strain.

The stop-tested specimens were then examined using ultrasound C-scan and microscopy for

evidence of damage at the points of strain increase. C-scans taken from the specimens (Fig. 7) show distributed damage that correlates well with the large strain increases that occurred in the high strain region around the hole.

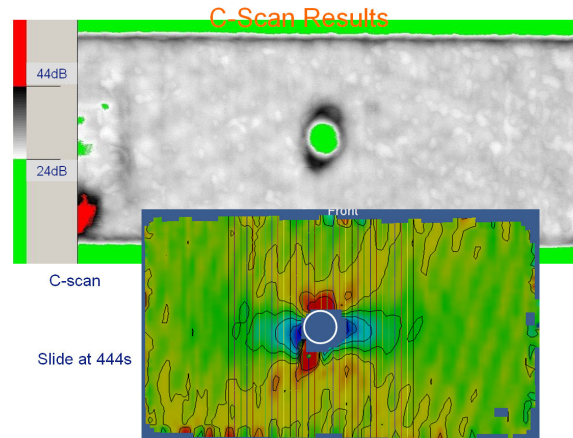


Fig. 7. Comparison of the strain field and C-scan taken at 444 secs shows correlation between damage surrounding the hole and large strain increases.

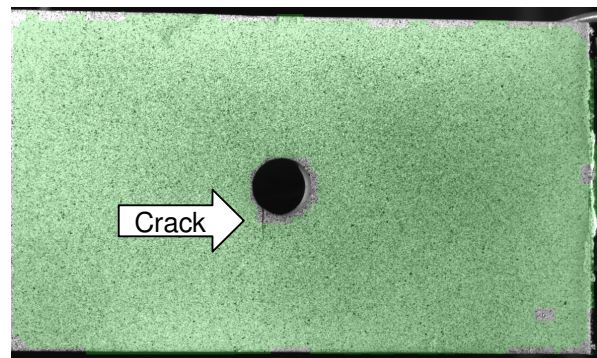


Fig. 8. Formation of a crack in the surface ply causes strain redistribution.

Microsections taken from the stop-test specimens at points of suspected damage (such as Fig. 9) show excellent correlation with predicted damage type, confirming the technique's ability to identify damage. It is also noted that microsections taken away areas of suspected damage did not exhibit damage.

The use of acoustic emission to identify and isolate damage mechanisms was also investigated. It was reported by Bailey et al [6] that composite damage mechanism could be successfully distinguished using variations in signal amplitude between high energy fibre damage and low energy matrix damage. This variation resulted in two peaks in the signal amplitude spectra that identified individual damage mechanisms (Fig. 10). Recorded

amplitudes and the amplitude spectrum are presented in Fig. 11 and Fig. 12 respectively. It was found that distinct damage distributions did not occur, preventing damage mechanisms from being isolated. Possible explanations for this are that the amplitude distributions resulting from individual damage modes are not statistically distinct, that the expected amplitude distributions occurred outside the limits of the acoustic emission equipment or that the amplitude distributions resulting from individual damage mechanisms were drowned out by the more frequent matrix damage and noise resulting from test machinery, traffic and other university activities. Efforts were made to isolate and filter background noise but were without success.

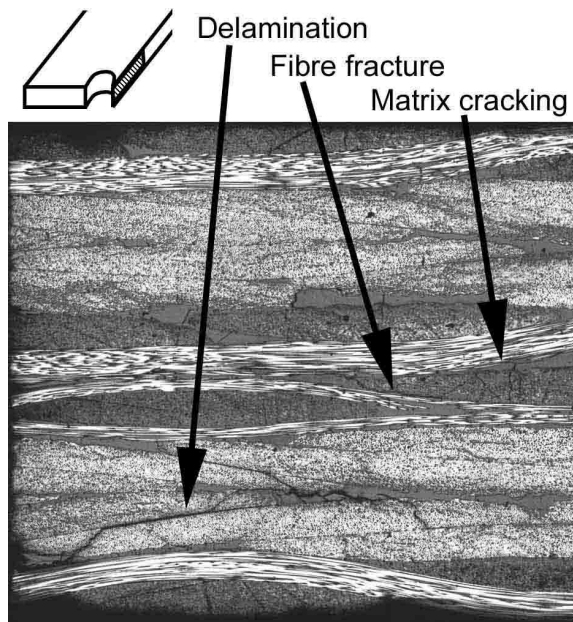


Fig. 9. Microsections confirm identified damage.

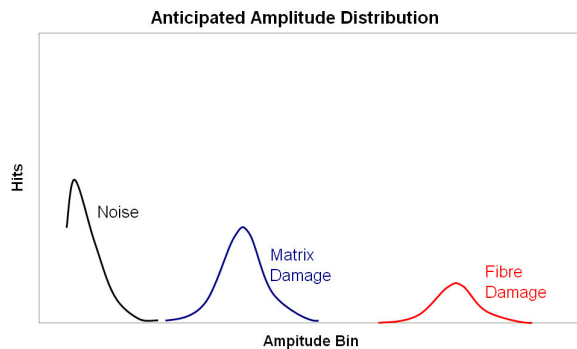


Fig. 10. Anticipated amplitude spectrum with peaks for individual damage mechanisms.

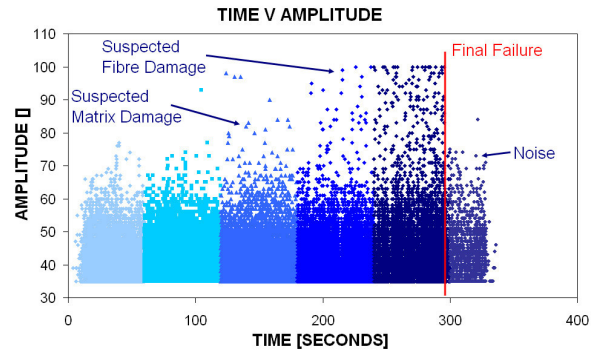


Fig. 11. Recorded signal amplitudes during test.

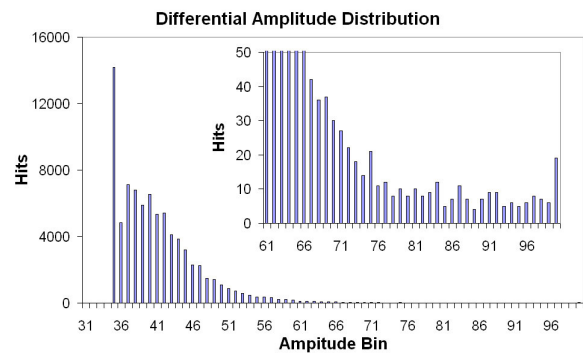


Fig. 12. Actual amplitude spectrum does not exhibit distinct peaks for individual damage mechanisms.

#### 4. Future Work

Tests will be repeated with 0/90° laminates to simplify results and isolate individual damage mechanisms. Additionally, more sophisticated acoustic emission equipment with better filtering and data processing capabilities has been obtained for use in the investigation.

#### 4. Conclusions

A strain field based method has been described for locating and identifying damage mechanisms in laminated composites. The technique has been shown to detect sub-surface damage by identifying sudden increases in strain resulting from changes in laminate compliance. Furthermore, individual damage mechanisms were successfully distinguished from the observed strain increases and confirmed using ultrasound C-scan and micrography. Acoustic emission was shown to be invaluable for indicating damage events but was not found to be successful as a means of identifying damage mechanism.

Overall, the described strain field method has proved to be an invaluable tool for locating and

identifying damage and has numerous applications in validating predictive failure models and for developing better understanding of composite damage behaviour.

**Acknowledgements**

The support of Bristol University, Airbus, Shorts, Hexcel, ESPRC, DTI and MOD is gratefully acknowledged.

**References**

[1] ASTM D5766/D5766M-95 “Standard Test Method for Open Hole Tensile Strength of Polymer Matrix Composite Laminates”, 1995  
 [2] Chalal, H., Meraghni, F., Avril, S., Pierron, F. “Experimental Identification of a Damage Model for Composites using the Grid Technique Coupled to the Virtual Fields Method”. *Proceedings of Composite Testing and Model Identification*, Bristol UK, Book of

Abstracts, pp 104-105, 2004.  
 [3] Zhang, D., Sandor, B.I., “Damage Evaluation in Composite Materials using Thermographic Stress Analysis”. *ASTM Special Technical Publication*, n 1122, pp 341-353, 1992.  
 [4] Ambu, R., Aymerich, F., Bertolino, F. “Investigation of the Effect of Damage on the Strength of Notched Composite Laminates by Digital Image Correlation”. *Journal of Strain Analysis for Engineering Design*, v 40, n 5, pp 451-61, 2005.  
 [5] Niklewicz, J., Sims, G. D. “The Use of Electronic Speckle Pattern Interferometry for Determining Non-Uniform Strain Fields”. <http://midas.npl.co.uk/midas/content/mn056.html> CMMT(MN)056, 1999.  
 [6] Bailey, C.D., Freeman, S.M., Hamilton, J.M., Jr. “Acoustic emission monitors damage progression in graphite epoxy composite structure”. *Materials Evaluation*, v 38, n 8, pp 21-71, 1980.

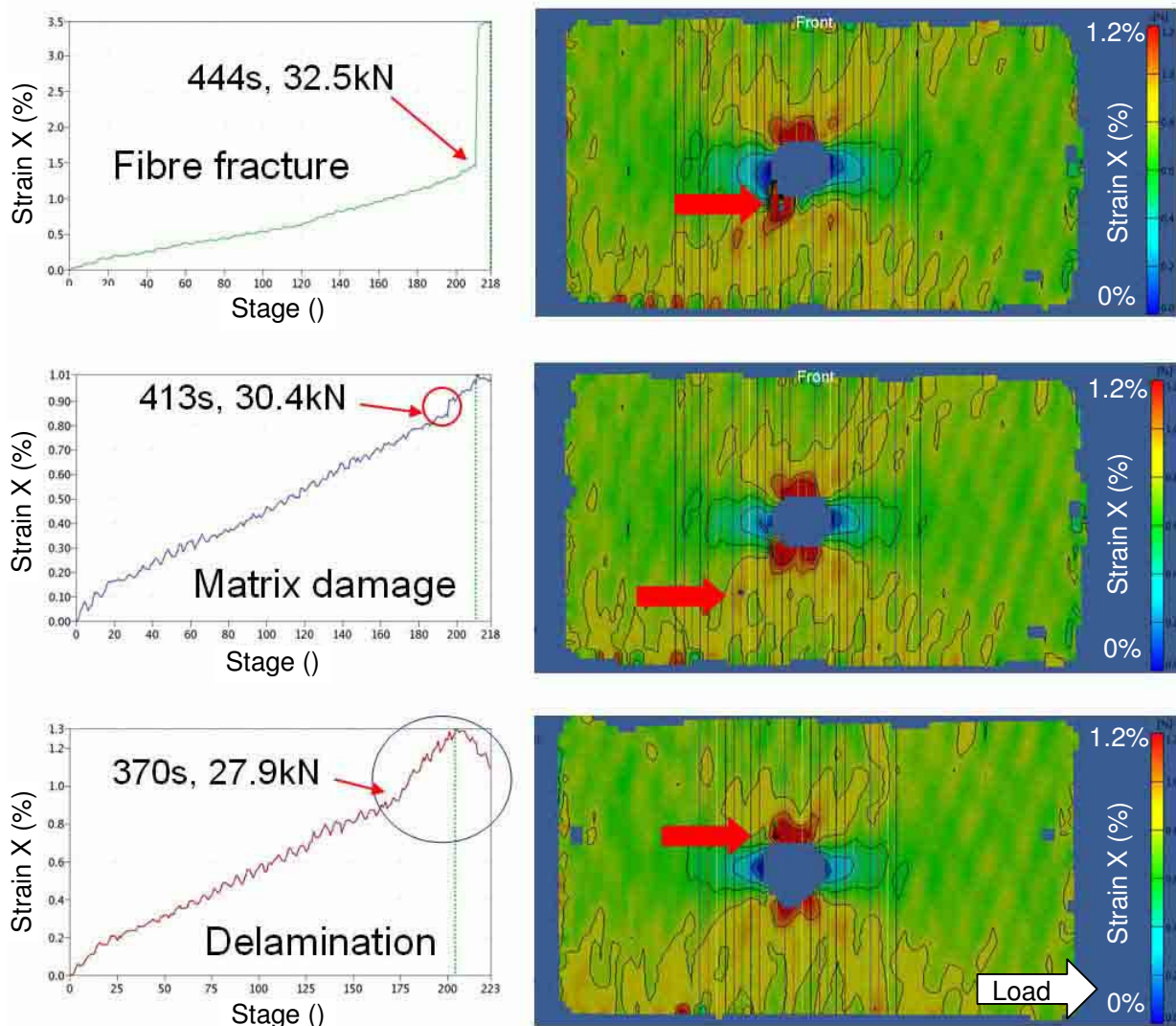


Fig. 13. Damage mechanisms identified by rate and magnitude of strain change.